Communications in Physics, Vol. 31, No. 1 (2021), pp. 1-22
DOI:10.15625/0868-3166/15547

REVIEW PAPER

SUPERCONTINUUM GENERATION IN PHOTONIC CRYSTAL FIBERS INFILTRATED WITH LIQUIDS

CAO LONG VAN[†]

Institute of Physics, University of Zielona Góra, Prof. Szafrana 4a, 65-516 Zielona Góra, Poland

[†]*E-mail:* caolongvanuz@gmail.com

Received 28 September 2020
Accepted for publication 14 October 2020
Published 5 January 2021

Abstract. *In this paper we present the development of a new direction in so-called optofluidics, namely the research of photonic crystal fibers (PCF) infiltrated with liquids. In particular we concentrate on the flagship application of PCF, the process of Supercontinuum Generation (SG), in which injected monochromatic pulse may be dramatically broadened (spectrally), which creates a coherent beam generation of high brightness comparable to that of monochromatic lasers. The supercontinuum is formed when a collection of nonlinear processes act together upon a pump beam in order to cause severe spectral broadening of the original pump beam. Explanation of this process is based on numerical simulations for Generalized Nonlinear Schrödinger equation (GNLSE) which describes the rich nonlinear dynamics of pulse propagation in nonlinear dispersive media. All nonlinear phenomena involved in SG will be analyzed. We present specially activity of the Polish-Vietnamese Group from the beginning in 2016 to recent time in this domain. Some recent scientific projects concerning fiber physics of our Group in the near future, especially applications in Biology and Medicine will be mentioned.*

Keywords: Photonic Crystal Fiber, Supercontinuum Generation, Generalized Nonlinear Schrödinger equation.

Classification numbers: 42.55.Tv; 88.60.np; 42.25.-p.

I. INTRODUCTION

Supercontinuum is a phenomenon based on a set of effects resulted from combined interaction of linear and nonlinear properties of optical medium involved in photonic crystal fibers (PCFs). The input monochromatic pulse of light is broadened spectrally to form a continuous spectrum in a beam of high brightness, even comparable to that of a monochromatic laser. The output spectrum becomes much wider than the input (Fig. 1).

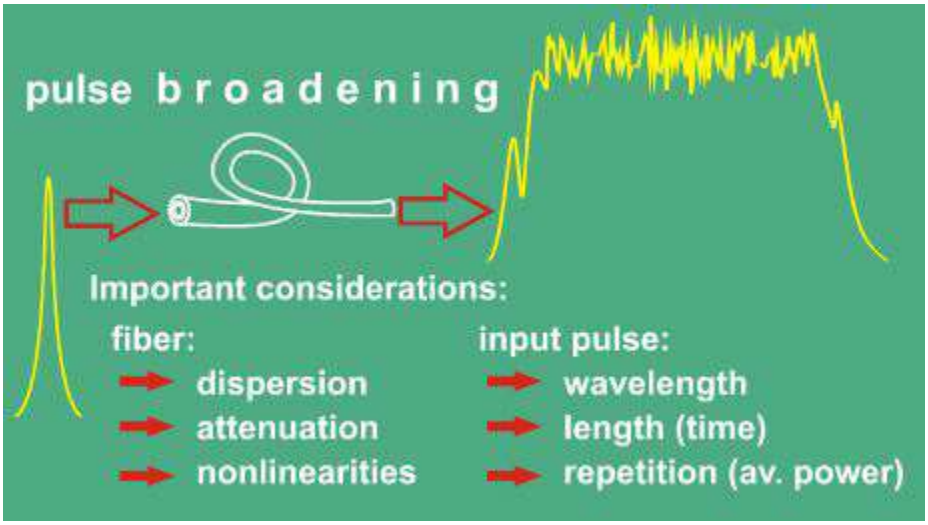

Fig. 1. Supercontinuum generation.

Discovery of the lasers realized experimentally by Maiman [1] for the first time in 1960 gives as a light source with very high intensity. This created a very important domain of physics, namely *nonlinear optics* [2]. To this time the majority of optical effects are considered only in the case of a linear material response of a medium to an incoming light field. However when the intense light field is high, nonlinear optical effects appear which dramatically modify properties of the incoming light. Experimental nonlinear optics started from the experiment on second harmonic generation performed in 1961 by Franken *et al.* [3]. In this experiment, two photons having the same frequency made up a photon of the doubled frequency by the nonlinear material responses of the medium. In this phenomenon, a light spectrum of an enormous broaden bandwidth was generated together with new frequency components, so one can say that a phenomenon, later called as Supercontinuum Generation (SG) has been observed there for the first time.

The further development of nonlinear optics provided to the appearance of *conventional optical fibers* which made the revolution not only in nonlinear optics but also in higher technologies as in telecommunication for last few decades. This discovery is treated as one of the greatest scientific advents in the XX century. A new field of physics appeared, namely *nonlinear fiber optics* [4]. This field had developed intensively, so new nonlinear phenomena were discovered, such as self-phase modulation in fibers [5] and parametric mixing processes [6, 7]. In particular optical solitons [8] and their dynamics [9, 10] have been highly interested by researchers. These

nonlinear phenomena played an important role in explanation of SG mentioned above. Now we have an ultra-broad spectrum spanning almost the complete visible region of light [11, 12].

Guiding of light in optical fibers based on the phenomenon of total internal reflection (TIR). A break point in development of optical fibers has been made in the 1950s by covering of glass fiber with a material with a lower refractive index [13,14]. This type of fiber structure including the core and cladding is used as the basic solution until now. Since the first experimental realization of low-loss optical fiber in 1970 [15], worldwide telecommunication experienced extraordinary growth.

However the conventional fiber guiding the light by TIR has several limits related to optical nonlinearities and attenuation. Several new guiding mechanisms minimizing these effects have been proposed. Among these mechanisms, discovery of *Photonic Crystal Fiber* (PCF) is a milestone in the development of fiber optics. This has been started by papers [16, 17] through extending band-gap mechanism in solid state physics to photonics. In 1991 the first experimental observation of the photonic band-gap effects has been demonstrated in Ref. [18]. Inspired by this paper, Russel and his collaborators fabricated the first PCF it by the method of stacking silica capillaries in a hexagonal pattern. The light guiding in the core is based the band-gap mechanism. The typical structure of the first PCF consists of micro-structured fibers made from silica glass with air-holes arranged in a hexagonal lattice with a solid core, named now solid-core photonic crystal fiber [19]. The central region was replaced by a glass rod acting as the core (see Fig. 2(a)).

The advantage of solid-core PCF in comparison with conventional fiber is that by changing its geometrical structure, namely the diameter and lattice pitch of air-holes in the cladding region, one can freely manages its dispersion (D). From other side, one can use various materials to moving the zero dispersion wavelength (ZDW) and also making modification of the dispersion's shape. A typical example that for the PCFs made of silica, the ZDW can be shifted into the visible region, in consequence a range of various pulse sources would be effectively used for generating broadband SC can cover both of the near-infrared and visible spectrum. It is available to achieve a large negative dispersion and ultra-flat or normal dispersion, which is essential for SG process in the required wavelength range.

In other paper [20] Russel and his coworkers tried to guide the light in the air-core (see Fig. 2(b)). The larger air core is now in the central region. PCF with this structure can confine more than 99% of the light in its core. It called later called hollow-core photonic crystal fiber (HC-PCF). It has a second name as photonic band-gap (PBG) fiber because of its guiding mechanism. Further studies showed that the exact structure of the cladding is not essential for obtaining broadband guidance [22, 23], but the geometry of the first layer surrounding the core is crucial for the transmission character of the fiber [24, 25]. Wang et al. experimentally demonstrated in Ref. [25] that loss of this fiber depends crucially on the core shape. A breakthrough to guide the light in the air-core fiber is achieved by Pryamikov *et al.* [26] when they fabricated a fiber with a single cladding layer and the core formed by a single row of silica capillaries (see Fig. 2(c)). In comparison with PBG-fibers, this fiber has relatively broader transmission windows in the mid-infrared range (MIR) and lower loss. It is named negative-curvature core fiber. This fiber is also called as anti-resonant (AR) fiber. The disadvantage of PBG fiber is that its attenuation is still not low enough for communication. Therefore, HC-PCFs are not suitable for data transmission for a long distance. However the large possibilities of modifying their structure, and thus their optical properties gave us many various applications not achieved by conventional ones. One can mention

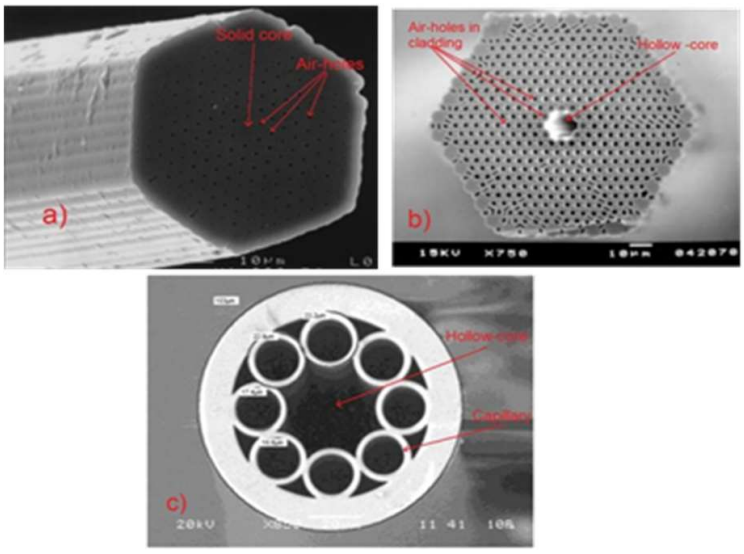

Fig. 2. Scanning electron microscope (SEM) images of (a) solid-core PCF [19], (b) PBG-fiber [20], (c) AR fiber [21].

some of them: a large mode area (LMA) HC-PCF used for high power delivery [27], HC-PCF with high birefringence [28] used to measure physical properties, while liquids and gases can be detected by the sensor using suspended core PCF [29]. With the flexible capability of modifying dispersion and mode area, HC-PCF is a most suitable for studying the nonlinear effects involved in SG [11].

Furthermore the use of different materials for making PCFs, for example heavy metal oxide glasses and tellurite which have much higher nonlinear coefficients than silica glasses, gives us more broadband transmission into the mid-infrared region [30]. This creates new possibilities for the fiber design. Reassuming, PCFs are powerful flexible tool for considering all optical effects. Furthermore they have many effective applications.

On other hand, one can infiltrate liquid into the core of HC-PCF. By varying the liquids' refractive index properly we can modify the guiding effect of the fiber from basing on modified total internal reflection to basing on the photonic band gap effects. In consequence, the optical characteristics of the fiber would highly depend on the temperature and concentration of liquids. Therefore by using liquids, the dispersion properties of the fiber can be further modified without changing its geometrical parameters by varying the temperatures and concentrations. One can say that insertion of liquids in PCFs introduces new degrees of freedom for observing and controlling nonlinear effects. In Sec. II, we will present in detail dispersion and its engineering in PCF infiltrated with liquids. Due to the unique properties of the liquid, e.g. high nonlinearity, high transparency, possibility of modifying the refractive index by changing ambient temperature, liquid core PCFs have numerous applications. We can mention some examples: the liquid core PCFs applied in e.g. sensing, laser, and SG; The AR fiber infiltrated with low-index liquid used for optofluidic laser [31] and as temperature sensors [32]...

My paper is organized as follows. In Sec. II, I will briefly present an important concept, namely the *dispersion* an how can modify it for different purposes, in other words how can make *dispersion engineering*. For this purpose Mode Solutions (MODE) simulation program provided by Lumerical to modelling PCF infiltrated with liquids for different applications, in particular for SG is used. I will not demonstrate this in detail here, concentrating only on analyzing SG in Sec. III. The last section contains conclusions.

II. DISPERSION AND ITS ENGINEERING IN PCF INFILTRATED WITH LIQUIDS

In this section, we describe briefly theory of propagating light in optical fibers. At first we start from linear propagation in standard step-index fibers for fixing some essential concepts, in particular the *dispersion.* Next, we consider the propagation in PCFs. Finally we extend this to nonlinear propagation which leads to *Generalized Nonlinear Schrödinger Equations* (GNLSE). In which, the characterized parameters and quantities of light propagating process are clearly mentioned.

A standard derivation of the NLSE in arbitrary dispersive media has been given in [33, 34]. A more detailed derivation for the case of optical fibers can be found in an excellent book [4], in which all nonlinear phenomena involved in the problem have been clearly described. If a source less medium is assumed, one that does not generate current, but can still exhibit attenuation and gain, from the system of Maxwell's equation one can arrive at the wave equation (see also Eq. (1) in Ref. [33]):

$$\nabla \times \nabla \times \mathbf{E} = \frac{1}{c^2}\frac{\partial^2 \mathbf{E}}{\partial t^2} - \mu_0 \frac{\partial^2 \mathbf{P}}{\partial t^2} = 0, \tag{1}$$

where c is the light's speed in vacuum and $c^2 = \frac{1}{\mu_0 \varepsilon}$

Generally, one can use a quantum mechanical to check the polarization P. But it is well known that when the frequency is near a medium resonance, the quantum treatment is necessary. But in our case we are far from medium resonances, so we can use Taylor's series for P as follows (Eq. (4) in [33]):

$$\tilde{\mathbf{P}} = \varepsilon_0 \left(\tilde{\chi}^{(1)} \oplus \tilde{\mathbf{E}} + \tilde{\chi}^{(2)} \oplus \tilde{\mathbf{E}}\tilde{\mathbf{E}} + \tilde{\chi}^{(3)} \oplus \tilde{\mathbf{E}}\tilde{\mathbf{E}}\tilde{\mathbf{E}} + \ldots + \tilde{\chi}^{(i)} \oplus \tilde{\mathbf{E}}^i \right). \tag{2}$$

here χ^i $(i = 1, 2, 3, \ldots)$ is i-th order of the material's electric susceptibility. In the further we will consider the fiber made by symmetric molecules SiO_2, the second order susceptibility $\chi^{(2)}$ vanishes because of $\mathbf{P}(-\mathbf{E}) = -\mathbf{P}(\mathbf{E})$. If we take only the third order nonlinear effects related to $\chi^{(3)}$, the polarization induction consists of linear and nonlinear part:

$$\mathbf{P}(\mathbf{r}, t) = \mathbf{P}_L(\mathbf{r}, t) + \mathbf{P}_{NL}(\mathbf{r}, t), \tag{3}$$

which are expressed correspondingly as:

$$\mathbf{P}_L(\mathbf{r}, t) = \varepsilon_0 \int_{-\infty}^{t} \chi^{(1)}(t - t')\mathbf{E}(\mathbf{r}, t')dt', \tag{4}$$

$$\mathbf{P}_{NL}(\mathbf{r}, t) = \varepsilon_0 \int\int \int_{-\infty}^{+\infty} \chi^{(3)}(t - t_1, t - t_2, t - t_3) \vdots \mathbf{E}(\mathbf{r}, t_1)\mathbf{E}(\mathbf{r}, t_2)\mathbf{E}(\mathbf{r}, t_3)dt_1 dt_2 dt_3, \tag{5}$$

Now we assume for simplicity that nonlinear polarization $\mathbf{P}_{NL}$ in Eq. (3) is only a small perturbation to the total polarization. This is reasonable because for silica fiber the nonlinear effects are relatively weak. Thus in the first step, we put $\mathbf{P}_{NL} = 0$ in equation (1). Then it becomes linear in E. Furthermore in the case of optical fibers we have propagation in an arbitrary direction, say Oz. Thus in the linear regime, the linear wave equation has the form [4]:

$$\frac{\partial^2 \tilde{\mathbf{E}}}{\partial \rho^2} + \frac{1}{\rho}\frac{\partial^2 \tilde{\mathbf{E}}}{\partial \rho^2} + \frac{1}{\rho^2}\frac{\partial^2 \tilde{\mathbf{E}}}{\partial \varphi^2} + \frac{\partial^2 \tilde{\mathbf{E}}}{\partial z^2} + n^2 k_0^2 \tilde{\mathbf{E}} = 0\,. \tag{6}$$

where $k_0 = \omega/c = 2\pi/\lambda$ and $\tilde{\mathbf{E}}$ is the Fourier transform of the electric field $\mathbf{E}(r,t)$. The general solution can be presented as superposition of waves propagating in the z-direction:

$$\tilde{\mathbf{E}}_z(r,\omega) = A(\omega)F(\rho)\exp(\pm im\varphi)\exp(i\beta z) \tag{7}$$

where A is normalization constant depending only on ω, m is an integer number and β is the *propagation constant* defined as:

$$\beta(\omega) = \left[n^2(\omega)k_o^2 - k^2(\omega)\right]^{1/2}. \tag{8}$$

The propagation constant β is one of the key parameters to describe the light propagation in the optical fiber. The values of β are different for individual modes and depends on the frequency (wavelength). They are determined from the following equation for F (frequently called as eigenvalue equation)

$$\frac{d^2F}{d\rho^2} + \frac{1}{\rho}\frac{dF}{d\rho} + \left(n^2k_0^2 - \beta^2 - \frac{m^2}{\rho^2}\right)F = 0. \tag{9}$$

This equation has been considered in many excellent books [35–37] for determining an important parameter characterizing arbitrary fibers, namely apart from the *relative core index differences*

$$\Delta = \frac{n_1 - n_2}{n_1} \tag{10}$$

the *normalized frequency* V is defined by

$$V = k_0 a (n_1^2 - n_2^2)^{1/2}, \tag{11}$$

where a is radius of the core and λ is wavelength. Thus the number of modes of a particular fiber per specific wavelength depends on its design parameters and is determined by so called *cut-off condition*: All other modes are beyond cut-off if the parameter $V < V_C$, where V_C is the smallest solution of $J_0 V_C = 0$ or $V_C \approx 2.405$. In practice fibers are designed to satisfy that V is close to V_C. The cut-off wavelength λ_C for single-mode fibers might be obtained with $k_0 = 2\pi/\lambda_C$ and $V = 2.405$ in Eq. (11), core radius should be below 2 μm for fiber to support a single mode in the visible region. Single mode fiber is commonly used to transmit over longer distances [38].

It is well-known from Newton's time that in light propagation through a medium, as in an optical fiber, different modes need different time to pass through a certain distance. The total dispersion of optical fiber defined as:

$$D_t = \sqrt{\tau_0^2 - \tau_i^2} \tag{12}$$

where τ_0, τ_i are the width of the input pulse and the output pulse, the unit is seconds [s]. Usually we are interested in pulse expansion per kilometer. Dispersion increases the width of the pulse, it is calculated in units of [ps /km].

For monochromatic light waves propagating along the waveguide in the z-direction (waveguide axis), these constant phases move with phase velocity:

$$v_p = \frac{dz}{dt} = \frac{\omega}{\beta}. \tag{13}$$

In practice, the light wave is not ideally mono-chromatic, there is a group of waves with frequencies near each other spreading so that the final form has a waveform. This group of waves propagates with *group velocity*:

$$v_g = \frac{\partial \omega}{\partial \beta}. \tag{14}$$

We have the following relation for Group velocity:

$$v_g = \frac{c}{n_g}$$

where

$$n_g = n_1 - \lambda \frac{dn_1}{d\lambda} \tag{15}$$

is called *group index.*

For short pulse propagation in a single mode fiber [33, 34], the wavelength dependence of the propagation constant $\beta\omega)$ is called *chromatic dispersion*, which causes the short light pulse to be broadened. Expanding $\beta\omega)$ into Taylor series around the central frequency ω_0 we obtain:

$$\beta(\omega) = \beta_0 + \beta_1(\omega - \omega_0) + \frac{1}{2}\beta_2(\omega - \omega_0)^2 + ..., \tag{16}$$

where:

$$\beta_m = \left(\frac{d^m \beta(\omega)}{d\omega^m}\right)_{\omega=\omega_o} \qquad (m = 0, 1, 2, \ldots). \tag{17}$$

The parameters β_1 and β_2 are related to the refractive index $n = n_1$ and its derivatives through the relations:

$$\beta_1 = \frac{1}{v_g} = \frac{n_g}{c} \tag{18}$$

$$\beta_2 = \frac{1}{2}\left(2\frac{dn}{d\omega} + \omega\frac{d^2 n}{d\omega^2}\right). \tag{19}$$

Thus from physical point of view, the envelope of an optical pulse moves at the group velocity, whereas the parameter β_2 represents dispersion of the group velocity and is responsible for pulse broadening. This phenomenon is known in literature as the *group-velocity dispersion* (GVD), and β_2 is the GVD parameter. The GVD is the change of the group velocity with frequency. The wavelength range is said to be *normal dispersion* regime when $\beta_2 > 0$. In this case, group velocity decreasing with increasing optical frequency. The wavelength corresponding to a value of $\beta_2 < 0$ is called the *anomalous dispersion* regime (group velocity increasing with increasing optical frequency). The wavelength where $\beta_2 = 0$ is referred to as the *zero-dispersion wavelength (ZDW)* (see Fig. 3).

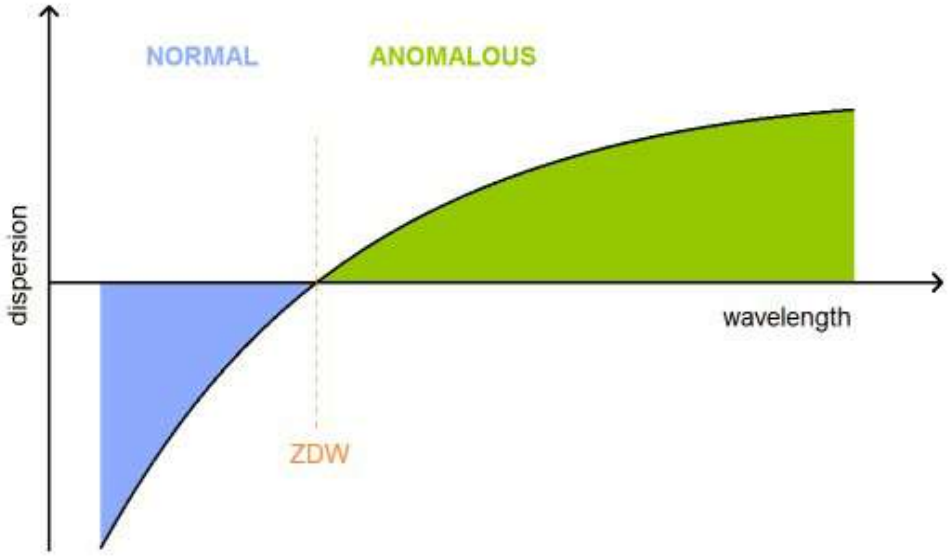

Fig. 3. Dispersion regimes in relation to the ZDW [39].

Another definition of the GVD is frequently used to describe the dispersion of fibers, namely the *parameter D*:

$$D = \frac{d\beta_1}{d\lambda} = -\frac{2\pi c}{\lambda^2}\beta_2 \approx \frac{\lambda}{c}\frac{d^2 n_{eff}}{d\lambda^2}. \tag{20}$$

It is expressed in units of ps/km/nm. According with Fig. 3, the region with $D < 0$ is normal dispersion, $D > 0$ ($\beta_2 < 0$) corresponds to anomalous dispersion regime and where $D = 0$, the wavelength is zero-dispersion wavelength (ZDW). The effects of higher-order dispersion will be taken into account when the very short pulses launch into the fiber or the central wavelength is very closed to the ZDW. The D of optical fiber depends on its geometrical structure and fiber material, and it is approximate to the sum of *waveguide dispersion* D_W and *material dispersion* D_M:

$$D = D_W + D_M \tag{21}$$

$D_W(\lambda)$ originates from the geometry of the fiber refractive index distribution that determines the D relation of the guided mode. D_M originates from the dependence of the refractive index of fiber material on the wavelength $n_{2g} = n_{2g}\lambda$, due to the difference in group velocities of different spectral components in the fiber. Pulse expansion due to material dispersion can be obtained by examining the group delay time in optical fiber [34]. The material dispersion D_M and the waveguide dispersion DW are given by the following formulas:

$$D_M = -\frac{2\pi}{\lambda^2}\frac{dn_{2g}}{d\omega} = \frac{1}{c}\frac{dn_{2g}}{d\lambda}, D_W = -\frac{2\pi\Delta}{\lambda^2}\left[\frac{n_{2g}^2}{n_2(\omega)}\frac{Vd^2(Vb)}{dV^2} + \frac{dn_{2g}}{d\omega}\frac{d(Vb)}{dV},\right] \tag{22}$$

where n_{2g} is the group index of the cladding material and V is given by Eq. (11), Δ is given by the Eq. (10) and $b = \frac{\beta/k_0 - n_2}{n_1 - n_2}$. The relation of (21) is presented on Fig. 4

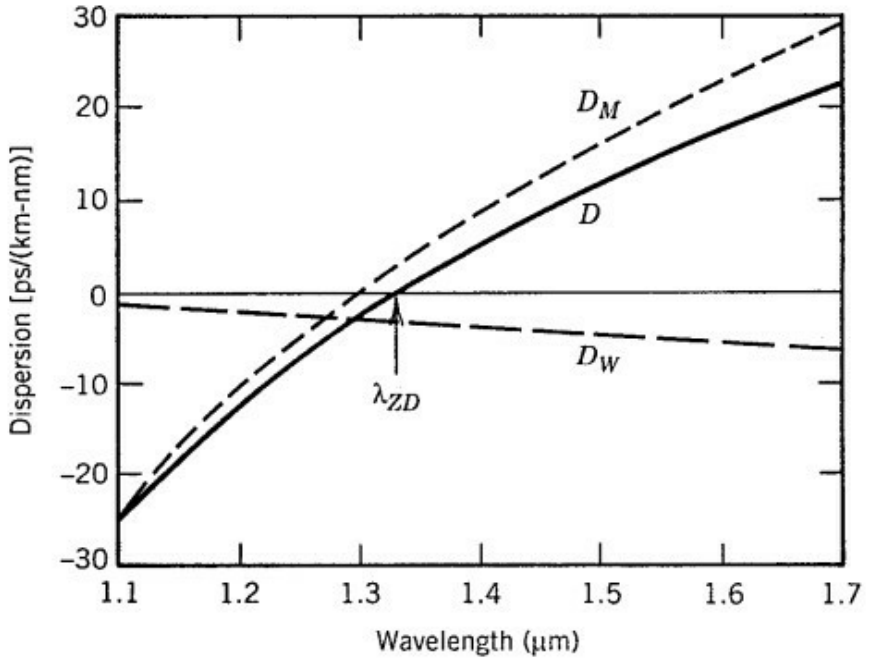

Fig. 4. Total dispersion $D$and relative contributions of material dispersion D_M and waveguide dispersion D_W for a single mode fiber [40].

As it has been recognized in Sec. I, Photonic fibers, thanks to the possibility of modification geometry, at the design stage, provide great freedom in designing dispersion properties for different purposes, for example it is possible to obtain a tailored spectrum of supercontinuum as we will see in Sec. III. Unfortunately, modifying the dispersion in the fabricated PCF is troublesome, it is difficult usually to manipulate its optical properties to make it a tunable optical device. Therefore, one can make a smooth change of dispersion properties of such fibers by filling them with gases or liquids. In this way, one can adjust the dispersion characteristics of PCF, in other words make engineering in PCF infiltrated with liquids. This enhances the range of its possible applications [40, 41].

Photonic Crystal is a periodic optical nanostructure designed to affect the motion of the photon in a similar way that the periodicity of a semiconductor crystal affects the motion of the electron. It is well-known that Photonic Crystals occur already in nature with various forms and have been studied for about 100 years. As it has been mentioned in Sec. I, Crystal Optical Fibers (PCF are new types of fiber, based on the properties of photonic crystals because they are capable of capturing light in the core area, what is not possible for conventional optical fibers). Some different kinds of PCF have been presented in Sec. I.

The PCF is basically a silica compound optical fiber in which there are holes or air holes running parallel to the fiber axis. Unlike conventional optical fibers, the core and cladding area of PCF are also made from the same material, and all properties of PCF are derived from the

presence of these air holes. Until now, the continuous development of fiber technology and its manufacturing industry for conventional fibers has reached its limit. The main advantage of PCFs over classic step-index fibers is the fact, that by adjusting the geometrical parameters of the photonic lattice, the waveguide dispersion can be designed with big freedom. Therefore PCF is an alternative fiber optic technology with many advantages in speed, bandwidth, bending ability, low dispersion, because one can control its behavior by modification of the shape, size and position of the holes or the air holes in the micro-structured cladding [42, 43]. The two basic geometrical parameters, namely hole diameter and hole spacing (or linear filling factor) lead not only to the guiding properties but also the dispersion, transmission and even nonlinear properties of PCF. In consequence PCF is the subject of intensive study since more than two decades and its many applications have been found in fiber lasers, optical amplifiers, high-power transmission lines, highly sensitive gas sensors and other nonlinear devices. The invention of PCFs makes a dramatic jump in communication technology. It not only overcomes the disadvantages of conventional optical fibers but also has outstanding advantages so that PCFs are increasingly studied, manufactured and widely used. The most common technique for the fabrication of PCFs is the *stack-and-draw method* [44] which is not presented in detail here.

The wave propagation in PCF is much more complicated in comparison with that in conventional optical fibers described briefly above. As with many other areas of scientific research, the software for computation and simulation of related problems is always the most effective tool for scientists to bring their designs closer to reality. In our simulation for PCF we use so-called *Mode Solutions (MODE)* simulation program provided by *Lumerical* [45]. This is a new (commercial with one-month free application) powerful optical simulation tool. Mode Solutions are beneficial for designing and analyzing any structured and geometric waveguide components. It is flexible in describing sophisticated geometrical devices, in particular suited for simulate microstructure optical fibers such as PCF, and optical waveguide integrated multiple layers. Mode Solutions is a new generation of design tools that incorporate advanced design features with innovative simulation tools. Mode Solutions' unique ability is to provide designers with flexibility in their project development process. Mode Solutions is designed for both general and advanced users. It is characterized by the simplicity and flexibility which are so needed to help designers quickly create a new photonic device. It simulates at the same time on multiple cores and multiple systems, the time domain calculation provides broadband results in a single simulation. Furthermore, it provides movies of dynamic simulations.

In numerical simulation, we must pay special attention to *single-mode light transmission*. In the results of the electromagnetic field spectral simulation we can see many different light modes that move in the core. We are interested only in the case, when the light confined in the core, in other words when we have only *fundamental mode*. Then propagation equation becomes one-dimensional as the GNSE presented below. If the requirement for light to run only in the fiber core area is not fulfilled, the light is wholly dispersed off the fiber and all results obtained by using GNSE are invalid. Of course this is only the first property of a PCF that we need to test. For obtaining final desired models for PCF we should look at the results that the Mode Solutions program has calculated in optimizing other properties of proposed models. In particular several aspects of the dispersion behavior have been analyzed as the zero-dispersion wavelength (ZDW) shift [46], the ultra-flattened dispersion characteristic [47], and the optimization of chromatic dispersion [48]. Mode Solutions program has also calculated two important parameters involved in

GNSE which is foundation for SG described in next section, namely *fiber loss* and *Effective Area* related to *Nonlinear Coefficient.*

During transmission of optical signals inside the fiber, there is some power loss. Consider a fiber of length L, if is P_{in} the input power launched of the fiber then the transmitted power P_{out} is given by:

$$P_{out} = P_{in}\exp(-\alpha L) \tag{23}$$

where the attenuation constantα is a measure of*total fiber losses* from all sources. In practice, α is usually expressed in unit of dB/km using the relation:

$$\alpha_{dB} = -\frac{10}{L}\log\left(\frac{P_{out}}{P_{in}}\right) \tag{24}$$

where L is the distance along the fiber and P_{out}/P_{it} is the ratio of output power to input power.

As it is emphasized above, during propagation of an intense laser pulse through a fiber, the response of the medium is both linear and nonlinear. In GNSE describing this propagation and used to considering Supercontinuum (SC) Generation in the next section, the *Nonlinear Coefficient* γ in $W^{-1}.km^{-1}$ is calculated by the following expression:

$$\gamma(\lambda) = \frac{2\pi n_2}{\lambda A_{eff}} \tag{25}$$

where n_2 is the nonlinear refractive index of silica ($2.66 \times 10?20$ m^2 /W) and A_{eff} is the *Effective Area* covered by the light during propagation through PCF. It is calculated by:

$$A_{eff} = \frac{\left(\iint |E|^2 dxdy\right)^2}{\iint |E|^4 dxdy} \tag{26}$$

In Ref. [41] we calculate numerically the refractive index, effective mode area and dispersion of the fundamental mode in the case when the air holes are filled with 11 organic solvents with unknown absorption losses and 6 with known absorption losses. A PCF based on the soft glass PBG-08 is designed and developed in the stack-and-draw process described above in Institute of Electronic Materials Technology in Warsaw. All considerations have been made by analyzing SEM images of real fiber. In particular we used our simulations for the case of toluene to SG consideration presented in the next section. In the paper [49], the HC PCF with a large core or 12 micrometer infiltrated with toluene was designed and developed. The large mode area is required for the efficient delivery of high power pulses from large mode area input fiber. After detailed useful presentation of state-of-the-art of experimental results on liquid core optical fiber SG, the authors reported for the first time an all-normal dispersion SG in a HC-PCF infiltrated with toluene. Dispersion properties of the proposed fiber were simulated and measured in a Mach-Zehnder interferometer setup. Next, the fiber has been used to SG (see below). Because toluene evaporates quickly in an open core fiber, continuous pumping as applied throughout the experiment.

We proposed in Ref. [50] a PCF made of fused silica glass and infiltrated with nitrobenzene. The guiding properties of considered fiber structure were determined numerically, namely estimated effective refractive index, attenuation, dispersion of the fundamental mode. From obtained results three structures were treated as optimal and they were chosen and used to SG.

Some of the liquids used in our simulations were highly toxic, so in real applications for example, although benzene and nitrobenzene which shift the ZDW the most, should be replaced by some alternatives, such as carbon tetrachloride, chroloform.

In Refs. [51,52] we proposed PCFs infiltrated with carbon tetrachloride, whereas in Ref. [53] with chloroform. In Ref. [51], the proposed PCF consists of eight rings of air-holes ordered in hexagonal lattice. It is made of fused silica glass and the central hole is filled with carbon tetrachloride. This liquid is transparent in a broad range of VIS and NIR wavelengths. Its refractive index is closed to that of fused silica, whereas the difference between these two materials is clear in the nonlinear refractive index. As usual, the guiding properties as effective refractive index, attenuation and dispersion of fundamental mode are determined numerically. From obtained results we optimized structures of PCF and in consequence two structures are chosen. They are verified in detail below in the next section against SG.

In Ref. [52] we considered a regular hexagonal lattice PCF with 5 rings air-holes. We studied theoretically an influence of its geometrical structure on dispersion properties of the fundamental mode using so-called the finite difference numerical method (FDM). In consequence we selected a proper model for the large-hollow core PCF. Then we fabricated this fiber using fused silica capillaries with standard stack-and-draw method described above. In the next, we have used a fusion splicer to close air holes in the photonic cladding as it has been made in our previous paper [51]. Then the fiber was mounted in a custom-made microfluidic reservoir filled with Carbon Tetrachloride. Dispersion characteristics have been calculated numerically and verified experimentally by Mach-Zehnder interferometer setup. The measured results match very well the simulated ones. The calculated confinement losses are similar to the losses of ideal structure, because material losses of Carbon Tetrachloride have dominant contribution and the waveguide losses are negligible. As in other models, we modelled SG with proposed PCF solving GNLSE by SSF method in the next section.

In our last published paper [54] two selected PCFs were analyzed two fibers with different structure parameters. The first one is the same as the fiber reported earlier in Ref. [52], while the second is a new one. Optimal PCFs are proposed with good nonlinear properties, and at the same time, they are easy to incorporate in all-fiber systems. A further analysis with SG for this selected PCFs will be made below.

The liquid used in Ref. [53] was chloroform. Among common nonlinear liquids chloroform has the lowest material dispersions in the visible region. Near- and mid-infrared wavelength ranges are convenient applications in novel areas because in this spectral region many substances have strong resonances associated with the fundamental rotational and vibrational resonances of various technologically vital molecules. Guiding properties of proposed PCF are again analyzed numerically. As a consequence two fibers were chosen. The nonlinear properties of selected fibers are simulated numerically by solving GNFSE using SSF method below.

Another interesting liquid with negligible toxicity is just water which is most common solvent used for biomolecules [55]. A temperature change of the water infiltrated PCF is interesting practical method for a fine tuning of ZDW. This new approach can be useful in applications in which fast dynamical compensation or dispersion shift is necessary. The influence of temperature on dispersion properties of proposed PCFs infiltrated with water has been considered in detail in Ref. [55]. We concluded that this type of fiber can be used for the precise adjustment of ZDW.

We consider also dispersion characteristics of crystal fibers infiltrated with water in an interesting structure, namely in a suspended-core SCF [56–58]. This is a special index guiding fiber type that consists of a suspended core fiber which leads to increase the core-cladding index contrast without using a second glass material. The cladding index is just decreased by the amalgamation of big air-holes. An example of such a fiber is shown in Fig. 5.

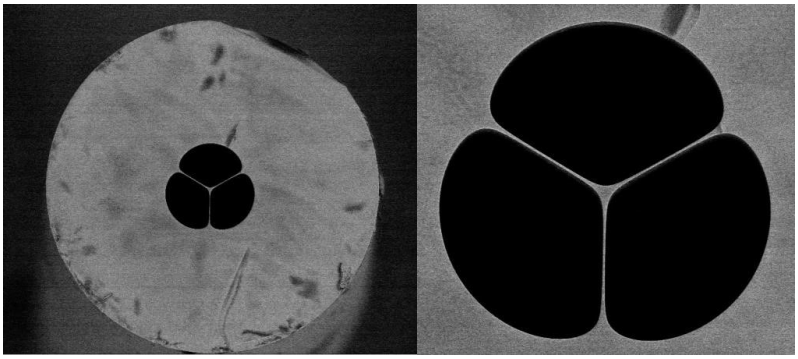

Fig. 5. The SEM of suspended core fiber NL_35B1. [59]

We have shown that [59] replacement of air with water improves dramatically the dispersion characteristic of the fibers: The *near-zero flat dispersion* can be achieved in the anomalous or normal dispersion region for various diameters of the core, what is valuable in the process of SG (see below). The changing the temperature of the fiber infiltrated with water leads to fine-tuning of the dispersion characteristics and this fiber could be suitable e.g. for spectroscopy applications. The SCF infiltrated with water can be modified further by adding organic components and biomolecules. Other enhancement of thermal dispersion tuning can be achieved if water is replaced by other organic liquids with higher thermal expansion coefficients and lower absorption.

In other our paper we replaced water by water-ethanol mixture [60]. Infiltration of the PCF with ethanol-water mixtures is very interesting for several reasons. It has very small viscosity, so it can penetrate very small holes. It is also nontoxic, and evaporation is very limited. In consequence ethanol-water mixture can be efficiently used for the PCF dispersion tuning with temperature and concentration. The proposed PCF is real and has been fabricated in ITME by stack and draw method described above. Results simulated numerically have been verified experimentally for several concentrations and temperatures of ethanol. Such verification has not been presented elsewhere. Our results allow for fine adjustment of fibers parameters e.g. to the wavelength of the pump used in SG.

A low-dispersion and low-nonlinearity silica PCF is designed and fabricated in Ref. [61]. The dispersion characteristics were measured and compared with calculated ones. They are well matched. In the next, we investigated femtosecond pulse propagation numerically by solving GNLSE and tested it experimentally. The results show that proposed PCF can be dedicated to near-infrared high-power femtosecond pulse delivery.

Recently interactions of light with the various cultured microorganisms, e.g., cells, bacteria, are studied and applied in bio-devices as bio-sensor [62] and optofluidic bio-laser [63, 64]. The aqueous solutions, which contain and produce the life function for organic elements, are called

buffer (buffer solution) or cell culture media (CCM). In Ref. [65] widely used buffers and CCM are studied, where we concentrated on optical properties as transmission, material dispersion and scattering properties. Well-fixed properties of buffers and CCM are essential for proper design of various optical sensors or other future optofluidic systems dealing with biological structures. In our paper, we have measured optical properties mentioned above for selected commercially available buffers and CCM. We concluded that although buffers and CCM with good optical properties can be used as optical medium for various bio-photonic systems, the long-term stability of these media should be taken into account. We observed their important change in properties after 8 months of storage. Therefore monitoring their optical properties is needed to identify degradation or infection in long-term considered experiments.

Reassuming, Mode Solutions (MODE) simulation program provided by Lumerical is an excellent power tool for modelling PCF infiltrated with liquids for different application purposes, in particular for its the most important application, namely for Supercontinuum Generation. This is the subject of the next section.

III. SUPERCONTINUUM GENERATION

Because in SG the nonlinearity plays an essential role, let us now go back to it. For the first order in Eq. (2), linear susceptibility, we just considered in previous section. The second order, that is quadratic susceptibility or quadratic nonlinearity, is responsible for a group of three-wave or three photon interaction processes, such as sum or difference frequency generation or second harmonic generation. But as we recognized before, the tensor elements of the quadratic susceptibility are non-zero only in optical media which have no inversion symmetry. An optical material is inversion symmetric if it gives the same response in any plane, in any direction of propagation. A glass is generally isotropic; therefore it exhibits inversion symmetry and no quadratic nonlinearity. That is why we do not observe second harmonic generation in glasses.

Now let's move to cubic nonlinearity – this describes interactions of four waves or four photons. Related processes are four wave mixing, optical Kerr effect, Raman scattering and third harmonic generation. These processes have been widely discussed in many text books [4, 33] and references cited therein). We concentrate on some of them [4].

In the first, we consider *self-phase modulation* (SPM). This is a manifestation of the optical Kerr effect. Since each wavelength in an optical pulse spectrum experiences different refractive index in dependence on the intensity at that wavelength, the phase delay will be introduced into the pulse's spectral components. This phase delay will have the same shape in the temporal domain, as the pulse optical intensity. Intensity dependent change of frequencies (Intensity dependent phase modulation) across the pulse leads to the change of spectrum of the pulse, but at the same time the pulse's temporal shape remains the same. SPM does not depend on GVD. Mathematically, SPM is described with the equation (27), which is demonstrates evolution of pulse amplitude along the propagation $A = A(z,t)$:

$$\frac{\partial A}{\partial z} = i\gamma A\,|A|^2\,. \tag{27}$$

The gamma is the nonlinear coefficient, which groups the nonlinear refractive index, frequency and effective mode area into one parameter and given by the formula (25). Nonlinear effect is known as *Cross-phase modulation* (XMP) in which the optical phase of a light wave is changed by the interaction with another light wave in a nonlinear medium like Kerr medium [4].

The nonlinear polarization appearing in media based on the nonlinearity term $\chi^{(3)}$ also contributes to making the description of XPM effects.

Now if we include both the nonlinearity term of SPM the effect of GVD in propagation equation (28):

$$\frac{\partial A}{\partial z} = -\frac{i\beta_2}{2}\frac{\partial^2 A}{\partial t^2} + i\gamma A|A|^2, \tag{28}$$

we will generate *solitons* [4,33]. Solitons (or solitary waves in optics) are such formations that do not change their shape during propagation due to the fact, that SPM and group velocity dispersion (GVD) effects can compensate or cancel each other out (Fig. **III**).

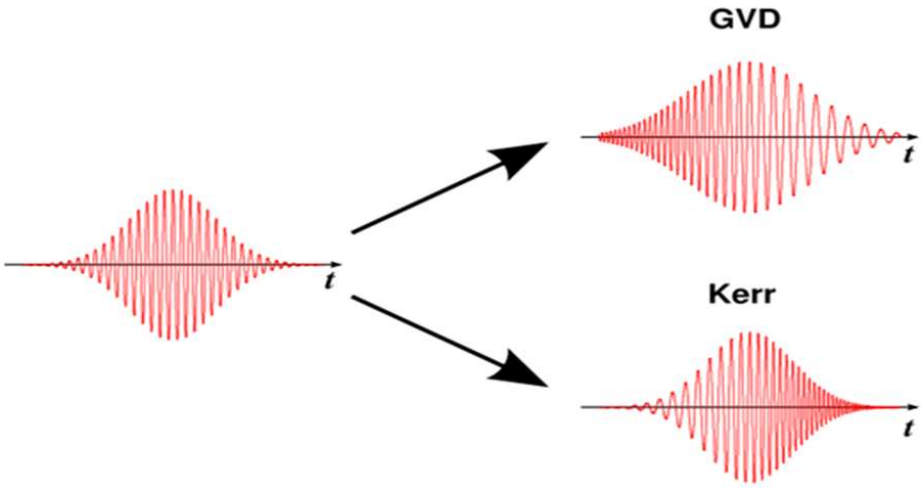

Fig. 6. Soliton as a result of complete compensation of SPM and GVD.

Depending on the order of the soliton, such structures can propagate without change of spectral or temporal shape, or they can fluctuate, periodically returning to their original form in PCF, as we see in the example taken from [8] (Fig. 7).

For comparison, this soliton has been already one year earlier simulated by Split-Step Fourier Method (mentioned below for numerical solving GNLSE), presented in Fig. 8 for one period [65].

The next interesting phenomenon is *four-wave mixing* (FWM) [4, 33]. In this process, interaction of two wavelengths can produce a pair of other two wavelengths. In a degenerate four wave mixing case, when two wavelengths out of four are the same, we have a process with three wavelengths (but still with four photons), where two pump photons produce one signal photon and one idler photon. Starting from dispersion relations, one can arrive at the phase-matching equation for four-wave mixing as follows [4]:

$$\kappa = 2\gamma P_0(1-f_R) + 2\sum_{m=1}^{\infty}\frac{\beta_{2m}}{2m!}\,\omega^{2m}. \tag{29}$$

By setting kappa to zero, such phase matching curves are obtained, which indicate where for a given pump wavelength, the signal and idler wavelengths would be located. FWM is a

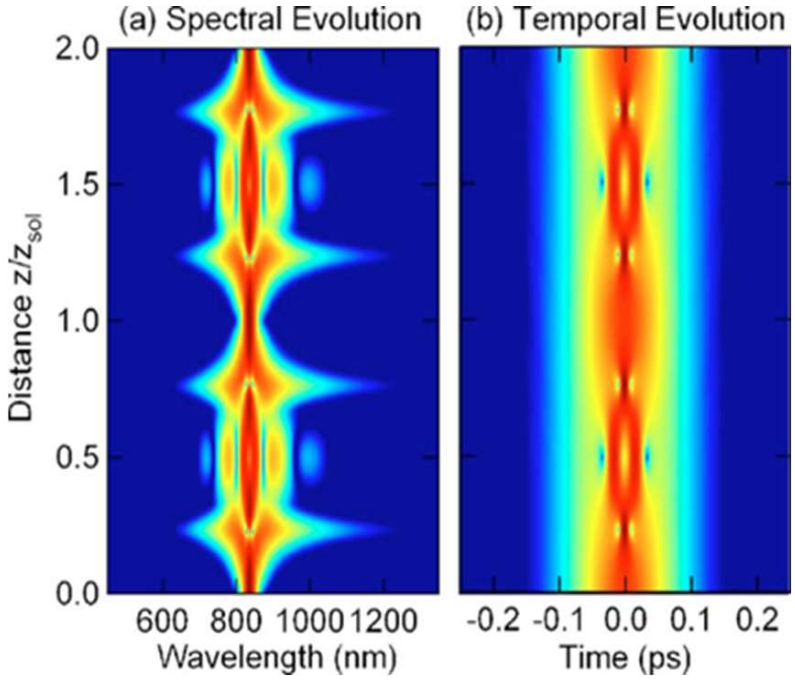

Fig. 7. Spectral and temporal shape of the third order soliton [8].

nonlinear optical process, which through the phase matching condition does depend on the linear phenomenon as dispersion. Mathematically, four-wave mixing is included along with SPM in the pulse propagation equation introduced below:

$$\frac{\partial A}{\partial z} = i \sum_{m \geq 2} \frac{i^m \beta_m}{m!} \frac{\partial^m A}{\partial t^m} + i\gamma A \left|A\right|^2 . \tag{30}$$

If anomalous dispersion is assumed starting just before the pump wavelength, we can observe a sudden break-up of the pulse envelope and red-shifting of solitons, which emerge in anomalous dispersion from the noise-seeded FWM [4]. This leads to modulation instability. Since this is one of major processes in formation of long-pulse pumped supercontinuum, one of the design strategies for nonlinear fibers, is optimization of dispersion profiles such, that this opening between the two parametric wavelengths be as widest as possible, or otherwise, depending on which is required.

Taking instead (7) the following form of solution of wave equation in frequency domain:

$$\tilde{E}(r, \omega - \omega_0) = F(x,y)\tilde{A}(z, \omega - \omega_0) \exp(i\beta_0 z) \tag{31}$$

we get following Generalized Nonlinear Schrödinger equation (GNLSE) [4, 33]

$$\frac{\partial A}{\partial z} + \frac{\alpha}{2} A - \sum_{k \geq 2} \frac{i^{k+1} \beta_k}{k!} \frac{\partial^k A}{\partial t^k} = i\gamma \left(1 + i\tau_{shock} \frac{\partial}{\partial t}\right) \left[A(z,t) \int_{-\infty}^{\infty} R(t') \left|A(z, t-t')\right|^2 dt' \right] . \tag{32}$$

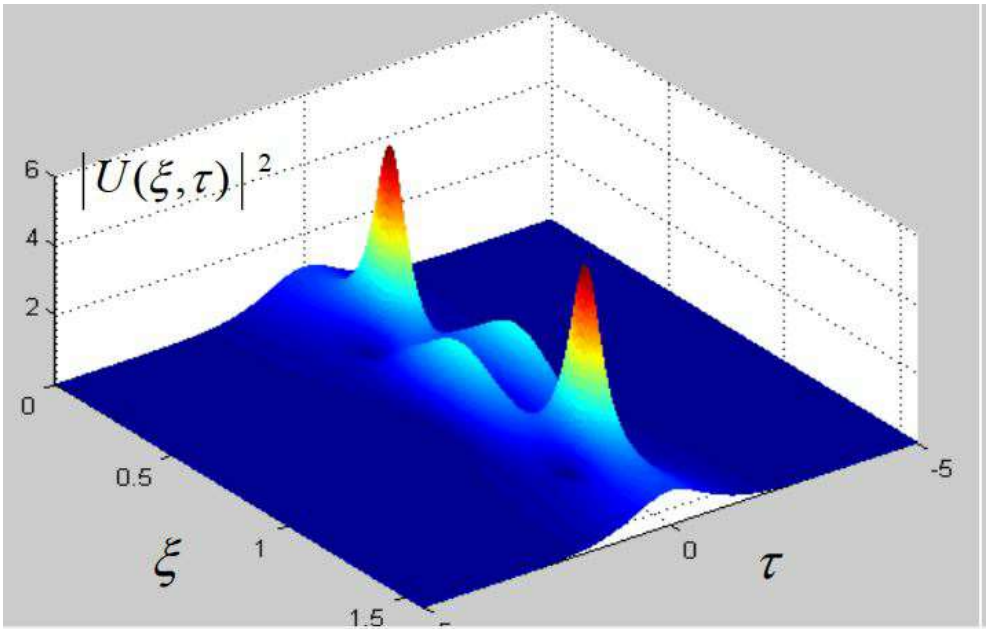

Fig. 8. Temporal shape of the third order soliton simulated in Ref. [66].

This important equation allows us to reconstruct the rich nonlinear dynamics of pulse propagation which contains, among others, all nonlinear phenomena mentioned above. In its left side, the second term describes fiber attenuation and the third represents fiber dispersion resulting from Taylor expansion (16) in frequency domain. They are linear effects involved in the process. Whereas the right side of equation (32) contains nonlinear effects [4, 33]. The *self-steepening* is a typical nonlinear process related to the dependence of intensity on the group index. Since there is a higher group index for the pulse peak than that for the pulse rest so the previous one travels with a lower velocity comparing to the later. In consequence, the intensity gradient of the leading edge decreases and that of trailing edge increases. Thus self-steepening of the pulse leads to the formation of a steep front in the trailing edge of the pulse, resembling the usual shock wave formation. From this reason this effect is called also the *optical shock.* The pulse becomes more asymmetric in the propagation and its tail finally breaks up. The cubic nonlinearities discussed above (SPM, XPM, FWM) and Raman scattering are other terms included in this side.

Thus after designing a nonlinear PCF and dispersion engineering in PCF infiltrated with liquids described in previous section, we know its dispersion characteristics, we can expect its attenuation, we know what the nonlinear refractive index and Raman response are, we can estimate what kind of nonlinear frequency conversion performance we could expect. For solving GNLSE (32), there several approximate analytical methods reviewed in Refs. [34, 67]. But this equation is so complex that it is usually solved numerically by so-called Split-Step Fourier (SSF) Methods described in Refs. [33, 66], in which linear and nonlinear effects treated separately over very short propagation distances.

Paper [41] starts for our consideration of SG by comparing the SG performance for the fiber structures with and without liquids using numerical solving GNLSE by SSF method. We restricted ourselves in this paper to the case when the PCF structure with air holes is filled with toluene and dispersion terms up to the ninth order. An extended study for SG in PCF with core filled with toluene has been performed in Ref. [68]. Two proper structures have been chosen. We have concluded that although confinement losses in the considered are as high as 0.4 dB/cm, the coherent SG in the range from 1.0 to 1.7 micrometer with the pulse energy conversion of 16% is feasible in 4 cm long fiber samples with standard fiber femtosecond lasers. A PCF proposed in Ref. [69], also infiltrated by toluene has been used to SG, which has been investigated numerically by solving GNLSE, and next verified experimentally with fiber sub-picosecond pulses for a range of pump energies. The coherence of the obtained supercontinuum has been also considered numerically with the uses of the first order coherence. The value of this coherence was equal 1 across the obtained spectrum. As it has been noted above, continuous toluene pump system was needed. The authors concluded that experimental and numerical results are in excellent agreement both in spectral width and shape of the spectrum.

We proposed in Ref. [69] a PCF infiltrated with nitrobenzene and by numerical analysis we obtained three optimal structures for SG. It was formed in the first centimeter of the light propagation. These fibers are good candidates for all-fiber SG sources as an attractive alternative to glass-core fibers, because the nonlinearity of nitrobenzene is much higher than that of silica. The proposed model may give us new low-cost all fiber systems for SG.

As it has been emphasized above, some of the liquids used in our simulations were highly toxic, so in real applications for example, although benzene and nitrobenzene which shift the ZDW the most, should be replaced by some alternatives, such as carbon tetrachloride, chloroform... Therefore we use now the proposed models PCF infiltrated by these liquids to considering SG. Firstly, we use two optimal structures chosen in Ref. [55] to SG. We used again numerical solutions of GNLSE based on SSF method. We concluded that the proposed PCF has some advantages over other types of optical fibers devoted to SG. Firstly, higher nonlinearity of Carbon Tetrachloride than fused silica leads to needed lower power of pulses required in SG, preserving at the same time the possibility of dispersion engineering to achieve a flat dispersion characteristic necessary in SG. Secondly, the proposed PCF can also be tuned by means of temperature to modulate the dispersion characteristic. Finally, Carbon Tetrachloride has similar refractive index of fused silica that as a filling medium it can easily incorporated in all-fiber optical systems.

The measured dispersion characteristics, wavelength-dependent losses and effective mode area obtained in the PCF described in [68] have been taken into account in GNLSE for considering SG. The temporal coherence of SG in the proposed PCF has been also calculated for the complex degree of first -order coherence according with the formula given in Ref. [70]. SG in this model was verified also experimentally. We concluded that the agreement between simulation and experiment is remarkably good. It certainly confirms the dominant role of single mode regime and all-normal dispersion features of observed SG dynamics.

Two fibers selected in Ref. [53] have been analyzed with respect to SG. It follows that both proposed fibers are good candidates for all-fiber SC sources as alternative to glass core fibers, because nonlinearity of chloroform is higher than silica and its toxicity is negligible. Two chosen fibers allow for SG on the basis of two mechanisms. The first one is SC in all-normal dispersion regime, so can be coherent. The second one is soliton fission based SC in anomalous regime.

In Ref. [59] some selected types of the suspended-core SCF infiltrated with water have been analyzed in the relation to SG. We have shown that in SCF made of borosilicate glass one can obtain flat dispersion characteristics which are required for efficient SG in fibers.

We demonstrate in Ref. [54] experimentally SG in PCFs with CCl4-filled cores when it is pumped with 90-fs-long pulses with a central wavelength of 1560 nm. Here we have used shorter pulses than previously to suppress the noise and to increase the temporal of the recorded SC pulses [71, 72]. We also used different pump wavelengths to better match the dispersion characteristics and the location of ZDW. In this way as it has been emphasized above, optimal PCFs are chosen with good nonlinear properties, and at the same time, they are easy to incorporate in all-fiber systems. Furthemore we demonstrate for the first time that this SC can be achieved in hollow-core fibers with CCl_4 infiltration and low-peak-power pulses. Evidently, the peak power of pump pulses used in this paper was 10 times smaller than that in our previous paper [52]. Moreover, it is extremely low in comparison to that in Ref. [73], where peak power was MW level. We used shorter input pulses than those in previous papers, and therefore the effects of polarization and laser noise on coherence degradation were reduced. As it has been shown by numerical analysis, the considered fibers have the potential for high coherence. The results obtained in Ref. [54] prove that the use of CCl_4-infiltrated PCFs is an interesting solution for compact all-fiber SG systems with low-power femtosecond lasers. We concluded also that a combination of low-cost, standard silica PCFs with cores infiltrated with CCl4 gives us possibility to develop efficient fibers with ultra-broadband transmission on short distances up to a few tens of cm. From the reason that the energy of the guided beams is confined in liquid cores, only a small fraction of light interacts with the silica walls in which it is highly attenuated. In consequence the work with liquid-core PCFs is challenging at the current stage, because it requires the use of dedicated reservoirs for input liquid. However, if silica fibers are used, all-fiber integrated systems are feasible to be constructed in the near future.

All PCF samples used in experiments were fabricated in Institute of Electronic Materials Technology (ITME) in Warsaw. As we know, the use of these liquids as cores in photonic fibers made it possible to obtain a medium with strong light location in a medium with high non-linearity over long distances. Initially, research work was theoretical, but after mastering the methods of controlled liquid introduction into photonic fiber cores (hollow core), they were confirmed by experimental research.

IV. CONCLUSIONS

As it is has been presented above, development of nonlinear optics and optical fibers created the nonlinear optical fibers [4]. This leads to the new model of optical fibers using photonic crystal claddings i.e. the dielectric matter with periodic structure of refractive index. This new kind of fibers, called later as photonic crystal fibers (PCFs) with special optical properties possible to be tailored with high degree of freedom. Furthermore they can be adjusted to the needs of experiment. The appearance of PCF in the late 1990s is considered as a revolution comparable with the invention of laser before. PCFs overcome many limitations intrinsic to step index fibers and create an ideal platform for observing new optical phenomena, in particular so-called supercontinuum generation (SG) which has reported for the first time in [74]. The big freedom in dispersion engineering of PCF allows SG to be performed optimally in the wide range of available pump sources, so one can use very short input pulses as well as high power continuous wave sources.

SG in PCF was immediately applied in many fields of science and technology. The freedom in dispersion tailoring is much more enhanced when PCF is filled by different liquids.

Recent studies of SG concentrate on giving new insight into the spectral broadening mechanism, adjusting supercontinuum properties to specific applications and creating new PCFs infiltrated by liquids suitable to SG through dispersion engineering of multicomponent glasses materials. Our work belongs to this trend of study.

A modern fiber optics laboratory has been created now in Vinh University. It can be used to carry out research in the field of non-linear fiber optics, fiber photonic systems and fiber optic sensors. We will design new kinds of PCFs, now infiltrated of new liquids and verify their optical properties, in particular their dispersion in this Laboratory. The first our paper with a complete experimental verification in our Laboratory has been already published [75].

ACKNOWLEDGEMENT

I would like to express my deep gratitude to Dr. Le Van Hieu for his wonderful job editing my manuscript and making it suitable for Communications in Physics.

REFERENCES

[1] T. H. Maiman, *Nature* **187** (1960) 493–494.
[2] J. A. Armstrong, N. Bloembergen, J. Ducuing and P. S. Pershan, *Phys. Rev.* **127,** (1962) 1918–1939.
[3] P. A. Franken, A. E. Hill, C. W. Peters and G. Weinreich, *Phys. Rev. Lett.* **7**, (1961) 118–119.
[4] G. P. Agrawal, *Nonlinear fiber optics*, fifth Edition, Elsever Academic Press (2013).
[5] C. Lin and R. H. Stolen, *Physical Review A* **17** (1978) 1448.
[6] R. H. Stolen, J. E. Bjorkholm and A. Ashkin, *Appl. Phys. Lett.* **24** (1974) 308.
[7] R. Stolen, *IEEE J. Quantum Electronics* **11** (1975) 100.
[8] J. M. Dudley, G. Genty, and S. Coen, *Rev. Modern Phys.* **78** (2006) 1135.
[9] A. V. Husakou and J. Herrmann, *Phys. Rev. Lett.* **87** (2001) 203901.
[10] J. P. Gordon, *Opt. Lett.* **11** (1986) 662.
[11] J. M. Dudley and J. R. Taylor, *Supercontinuum generation in optical fibers*, *Cambridge University Press*, 2010.
[12] R. R. Alfano, *The Supercontinuum Laser Source*, Springer, Berlin, 2006.
[13] A. C. S. van Heel, *Nature* **173** (39), (1954).
[14] H. H. Hopkins, N. S. Kapany, *Nature* **173** (39), (1954).
[15] F. P. Kapron, D. B. Keck, R. D. Maurer, *Appl. Phys. Lett*. **17** (1970) 423.
[16] S. John, *Phys. Rev. Lett.* **58** (1987) 2486.
[17] E. Yablonovitch, *Phys. Rev. Lett*. **58** (1987) 2059.
[18] E. Yablonovitch, T. J. Gmitter and K. M. Leung, *Phys. Rev. Lett.* **67** (1991) 2295.
[19] C. Knight, T. A. Birks, P. St. J. Russell, D. M. Atkin, *Opt. Lett.* **21**(19), (1996) 1547.
[20] R. F. Cregan, B. J. Mangan, J. C. Knight, T. A. Birks, P. St. J. Russell, P. J. Roberts, D. C. Allan, *Science* **285** (1999) 1537.
[21] A. D. Pryamikov, A. S. Biriukov, A. F. Kosolapov, V. G. Plotnichenko, S. L. Semjonov and E. M. Dianov, *Opt. Express* **19**(2011) 1441.
[22] S. Février, B. Beaudou and P. Viale, *Opt. Express* **18** (2010) 5142.
[23] F. Couny, P. J. Roberts, T. A. Birks and F. Benabid, *Opt. Express* **16** (2008) 20626.
[24] A. Argyros and J. Pla, *Opt. Express* **15** (2007) 7713.
[25] Y. Y. Wang, N. V. Wheeler, F. Couny, P. J. Roberts and F. Benabid, *Opt. Lett.* **36** (2011) 669.
[26] A. D. Pryamikov, A. S. Biriukov, A. F. Kosolapov, V. G. Plotnichenko, S. L. Semjonov and E. M. Dianov, *Opt. Express* **19** (2011) 1441.
[27] NKT Photonics, LARGE MODE AREA PHOTONIC CRYSTAL FIBERS, https://www.nktphotonics.com/lasers-fibers/product/large-mode-area- photonic-crystal-fibers/

[28] A. Ortigosa-Blanch, J. C. Knight, W. J. Wadsworth, J. Arriaga, B. J. Mangan, T. A. Birks, P. St. J. Russell, *Opt. Lett.* **25** (2000) 1325.
[29] A. S. Webb, F. Poletti, D. J. Richardson, J. K. Sahu, *Opt. Eng.* **46** (2007) 010503.
[30] R. Buczynski, H. T. Bookey, D. Pysz, R. Stepien, I. Kujawa, J. E. McCarthy, A. J. Waddie, A. K. Kar and M. R. Taghizadeh, *Laser Phys. Lett.* **7** (2010) 666.
[31] Y. Liu, Y. Wang, Z. Wang, X. Zhang, X.Liu, S. Gao, X. Wang and Pu Wang, *Nanophotonics* **7** (2018) 1307.
[32] C. Wei, J. T. Young, C. R. Menyuk and J. Hu, *OSA. Continuum.* **2** (2019) 2123.
[33] C. L. Van, *Comm. Phys.* **26** (2016) 301.
[34] C. L. Van, *Rev. Adv. Mater. Sci.* **23** (2010) 8.
[35] Y. R. Shen, *Principles of nonlinear optics*, Wiley, New York, 1984, Chap. 1.
[36] M. Schubert and B. Wilhelmi, *Nonlinear optics and quantum electronics*, Wiley, New York, 1986, Chap. 1.
[37] P. N. Butcher and D. N. Cotter, *The elements of nonlinear optics*, Cambridge University Press, Cambridge, UK, 1990, Chap. 2.
[38] M. Ebnali-Heidari, Majid & Dehghan, F & Saghaei, Hamed & Koohi-Kamali, Farshid & Moravvej-Farshi, Mohammad, *J. Modern Opt.* **59** (2012) 1384-1390.
[39] Le Van Hieu, *PhD Thesis*, University of Zielona Góra, 2018.
[40] G. P. Agrawal, *Fiber-optic communications systems*, Third Edition, ISBNs: 0-471-21571-6 (Hardback); 0-471-22114-7 (Electronic).
[41] J. Pniewski, T. Stefaniuk, H. L. Van, V. C. Long, C. V. Lanh, R. Kasztelanic, G. Sêpniewski, A. Ramaniuk, M. Trippenbach, R. Buczyñski, *Applied Optics* **55**(19) (2016) 5033-5040.
[42] J. C. Knight, *Nature* **424** (2003) 847-851.
[43] C. M. Smith, N. Venkantaraman, M.T. Gallager, D. Mueller, J. A. West, N. F. Borreili, D. C. Allan and K. W. Koch, *Nature* **424** (2003) 657.
[44] D. Pysz, I. Kujawa, R. Stepien, M. Klimczak, A. Filipkowski, M. Franczyk, L. Kociszewski, J. Buzniak, K. Harasny and R. Buczynski, *Bull. Pol. Ac.: Tech.* **62** (2014) 2300.
[45] https://www.lumerical.com/products/mode/.
[46] A. Fernando, E. Silvestre, P. Andres, J. J. Miret and M. V. Andres, *Opt. Express* **9** (2001) 687.
[47] W. H. Reeves, J. C. Knight, P. St. J. Russell and P. J. Roberts, *Opt. Express* **10** (2002) 609.
[48] K. Saitoh, M. Koshiba, T. Hasegawa and E. Sasaoka, *Opt. Express* **11** (2003) 843.
[49] V. T. Hoang, R. Kasztelanic, A. Anuszkiewicz, G. Stêpniewski, A. Filipkowski, S. Ertman, D. Pysz, T. Woliñski, K. D. Xuan, M. Klimczak, R. Buczñski, *Optical Materials Express* **8**(11) (2018) 3568.
[50] L. C. Van, V. T. Hoang, V. C. Long, K. Borzycki, K. D. Xuan, V. T. Quoc, M. Trippenbach, R. Buczñski, J. Pniewski, *Laser Phys.* **30** (2020) 035105.
[51] Q. H. Dinh, J. Pniewski, V. H. Le, A. Ramaniuk, V. C. Long, K. Borzycki, K. D. Xuan, M. Klimczak, R. Buczyñski, *Applied Optics* **57**(15) (2018) 1.
[52] V. T. Hoang, R. Kasztelanic, A. Filipkowski, G. Stêpniewski, D. Pysz, M. Klimczak, S. Ertman, V. C. Long, T. R. Woliñski, M. Trippenbach, K. D.Xuan, M. Śmietana, R. Buczyñski, *Opt. Mater. Express* **9** (2019) 2264.
[53] L. C. Van, V. T. Hoang, V. C. Long, K. Borzycki, K. D. Xuan, V. T. Quoc, M. Trippenbach, R. Buczñski and J. Pniewski, *Laser Physics* **29**(7) (2019) 1.
[54] V. T. Hoang, R. Kasztelanic, G. Stêpniewski, K. D. Xuan, V. C. Long, M. Trippenbach, M. Klimczak, R. Buczyñski and J. Pniewski, *Appl. Opt.* **59** (2020) 1559.
[55] Q. H. Dinh, H. L. Van, K. D. Xuan, R. Kasztelanic, V. C. Long, Q. H. Quang, L. C. Van, L. M. Van, T. T. Doan and R. Buczñski, *dvances in Optics Photonics Spectroscopy & Applications IX, Publishing House for Science and Technology*, 978-604-913-578-1 (2017).
[56] K. D. Xuan, L. C. Van, V. C. Long, Q. H. Dinh, L. V. Xuan, M. Trippenbach, R. Buczñski, *Appl. Opt.* **56** (2017) 1012.
[57] A. S. Webb, F. Poletti, D. J. Richardson, J. K. Sahu, *Opt. Eng.* **46** (2007) 1.
[58] I. Savelii, J. C. Jules, G. Gadret, B. Kibler, J. Fatome, M. E. Amraoui, N. Manikandan, X. Zheng, F. Désévédavy, J. M. Dudley, J. Troles, L. Brilland, G. Renversez and F. Smektala, *Opt. Mater.* **33** (2011) 1661.
[59] K. D. Xuan, L. C. Van, V. C. Long, Q. H. Dinh, L. V. Xuan, M. Trippenbach and R. Buczyñski, *Appl. Opt.* **56** (2017) 1012.

[60] V. H. Le, R. Buczyñski, V. C. Long, M. Trippenbach, K. Borzycki, A. N. Manh, R. Kasztelanic, *Opt. Commun.* **407** (2018) 417.
[61] V. T. Hoang, B. Siwicki, M. Franczyk, G. Stêpniewski, V. H. Le, V. C. Long, M. Klimczak, R. Buczñski, *Opt. Fiber Tech.* **42** (2018) 119.
[62] L. Shao, Z. Liu, J. Hu, D. Gunawardena and H.-Y. Tam, *Micromachines* **9** (2018) 145.
[63] M. C. Gather and S. H. Yun, *Nat. Photon*. **5**(7) (2011) 406.
[64] X. Fan and S.-H. Yun, *Nat. Methods.* **11** (2014) 141.
[65] V. T. Hoang, G. Stêpniewski, K. H. Czarnecka, R. Kasztelanic, V. C. Long, K. D. Xuan, L. Shao, M. Śmietana, R. Buczyñski, *Appl. Sci.* **9** (2019) 1.
[66] Nguyen Viet Hung, *Propagation of light pulses in dispersive nonlinear media*, Master Thesis, Vinh University 9/2005 (in Vietnamese).
[67] C. L. Van and P. P. Goldstein, University of Zielona Góra, 2008.
[68] L. C. Van, A. Anuszkiewicz, A. Ramaniuk, R. Kasztelanic, K. D. Xuan, V.C. Long, M. Trippenbach, R. Buczyñski, *J. Opt.* **19** (2017) 125604.
[69] L. C. Van, V. T. Hoang, V. C. Long, K. Borzycki, K. D. Xuan, V. T. Quoc, M. Trippenbach, R. Buczñski, J. Pniewski,*Laser Phys.* **30** (2020) 035105.
[70] J. M. Dudley, S. Coen, *Opt. Lett.* **27** (2002) 1180.
[71] B. Gonzalo, R. D. Engelsholm, M. P. Sørensen and O. Bang, *Sci. Rep.* **8**, (2018) 6579.
[72] E. Genier, P. Bowen, T. Sylvestre, J. M. Dudley, P. Moselund and O. Bang, *J. Opt. Soc. Am. B.* **36** (2019) A161.
[73] A. Bozolan, C. J. S. de Matos, C. M. B. Cordeiro, E. M. dos Santos and J. Travers, *Opt. Express* **16** (2008) 9671.
[74] J. K. Ranka, R. S. Windeler, and A. J. Stentz *Opt. Lett.* **25** (2000) 796.
[75] T. C. Le, T. V. Hoang, H. V. Le, D. Pysz, L. V. Cao, T. D. Bui, D. T. Nguyen, Q. D. Ho, M. Klimczak, R. Kasztelanic, J. Pniewski, R. Buczyñski and K. X. Dinh, *Opt. Mater. Express* **10** (2020) 1733.